

Extracellular Matrix Expression and Production in Fibroblast-Collagen Gels: Towards an *In Vitro* Model for Ligament Wound Healing

STEPHANIE M. FRAHS,^{1,2} JULIA THOM OXFORD,^{1,2} ERICA E. NEUMANN,³ RAQUEL J. BROWN,²
CYNTHIA R. KELLER-PECK,² XINZHU PU,² and TREVOR J. LUJAN³

¹Biomolecular Sciences Graduate Program, Boise State University, Boise, ID, USA; ²Biomolecular Research Center, Boise State University, Boise, ID, USA; and ³Department of Mechanical & Biomedical Engineering, Boise State University, 1910 University Drive, Boise, ID 83725-2085, USA

(Received 1 February 2018; accepted 25 May 2018)

Associate Editor Jennifer West oversaw the review of this article.

Abstract—Ligament wound healing involves the proliferation of a dense and disorganized fibrous matrix that slowly remodels into scar tissue at the injury site. This remodeling process does not fully restore the highly aligned collagen network that exists in native tissue, and consequently repaired ligament has decreased strength and durability. In order to identify treatments that stimulate collagen alignment and strengthen ligament repair, there is a need to develop *in vitro* models to study fibroblast activation during ligament wound healing. The objective of this study was to measure gene expression and matrix protein accumulation in fibroblast-collagen gels that were subjected to different static stress conditions (stress-free, biaxial stress, and uniaxial stress) for three time points (1, 2 or 3 weeks). By comparing our *in vitro* results to prior *in vivo* studies, we found that stress-free gels had time-dependent changes in gene expression (col3a1, TnC) corresponding to early scar formation, and biaxial stress gels had protein levels (collagen type III, decorin) corresponding to early scar formation. This is the first study to conduct a targeted evaluation of ligament healing biomarkers in fibroblast-collagen gels, and the results suggest that biomimetic *in-vitro* models of early scar formation should be initially cultured under biaxial stress conditions.

Keywords—Cellular collagen gels, Mouse embryonic fibroblasts, Proteomics, Gene expression, Biaxial stress, Uniaxial stress, Confocal microscopy.

INTRODUCTION

Ligament and tendon tears are common injuries that result in over seven million hospital visits per year in the United States.¹⁰ After injury, ligament wound

healing follows a sequence of events that results in cell activation and the production and remodeling of the extracellular matrix.⁴³ Fibroblasts are the primary cells that create and modify the ligamentous scar tissue, a fibrous type I collagen network that provides structural integrity to the wound site after injury. However, scar tissue has inferior mechanical strength compared to healthy ligament,²³ and consequently there is a high incidence of recurrent sprains, with up to 30% of patients experiencing significant symptoms 3 years after a ligament injury.⁴⁶ In order to develop clinical techniques that improve the structural and functional restoration of torn ligament, the factors that influence remodeling must be identified.

One challenge to identifying these factors is the absence of an *in vitro* model to study fibroblast activation during ligament wound healing. Collagen type I hydrogels seeded with cells have emerged as a promising model for wound healing since they allow for the three-dimensional culture of cells in a defined extracellular environment, with varying degrees of static and temporal control. Previous studies have examined using collagen scaffolds seeded with fibroblasts for cell transplantation¹¹ and for attempting to recreate natural healthy ligament tissue.^{12,27} While progress has been made in using cellular gels to study tendon disease,¹⁶ cellular gels have not been used to study wound healing in ligament. The establishment of a biomimetic *in vitro* model system for ligament healing could enable a better understanding of the mechanical and chemical factors that promote the structural repair of the extracellular matrix and thereby strengthen injured ligament.

Address correspondence to Trevor J. Lujan, Department of Mechanical & Biomedical Engineering, Boise State University, 1910 University Drive, Boise, ID 83725-2085, USA. Electronic mail: trevorlujan@boisestate.edu

Essential matrix molecules that must be considered when establishing an *in vitro* model of ligament wound healing include collagen type I, collagen type III, collagen type V, decorin, tenascin-C, and the cell surface receptor integrin $\alpha 5$. Ligament wound healing initiates with fibroblast production of collagen type III and then shifts to production of collagen type I as the wound matures.^{4,8,33} Collagen fibrillogenesis in healing ligament is regulated by both increased levels of collagen type V protein,³⁵ and decreased levels of decorin proteins.^{8,38} Fibroblast migration to the wound site may be helped by increased levels of both tenascin-C¹³ and integrin $\alpha 5$ proteins.⁴² Although prior studies have evaluated the expression and production of some of these biomarkers in three-dimensional cellular gels,^{24,28,37} a comprehensive targeted analysis of these ligament wound healing biomarkers in cellular gels has not yet been conducted.

An *in vitro* model for ligament wound healing must also reproduce the structural organization of the collagen network. After ligament injury, the collagen network is initially highly disorganized, achieving only modest collagen alignment once remodeled into scar tissue.¹⁷ In contrast, native ligament is often highly organized, where collagen type I aligns along a preferred axis to resist forces along the load bearing direction. These differences in collagen alignment are likely associated with scar tissue regaining only 30–40% of normal ligament strength.^{18,20,44} Restoring this native alignment is critical to improving the strength and durability of healing ligament.²⁹ Therefore, a successful *in vitro* model for ligament wound healing should replicate the disorganized collagen network of early scar tissue. The collagen organization of three dimensional gels can be reliably controlled by modifying the static loading environment during culture, yet the effect of collagen organization on the cellular activity in these cell culture models is currently unclear.¹

The objective of this study is to measure the expression and production of the aforementioned matrix molecules in fibroblast-collagen gels that are subjected to different static loading environments. Our hypothesis is that fibroblasts cultured within disorganized collagen fiber networks will express and produce biomarkers more similar to healing ligament than fibroblasts cultured within aligned collagen fiber networks. Results from this study will be compared to previous *in vivo* research on ligament wound healing to determine whether our biomimetic constructs warrant further investigation as an *in vitro* model for ligament wound healing.

MATERIALS AND METHODS

Overview

Collagen type I gels, seeded with NIH-3T3 mouse embryonic fibroblasts, were maintained under three static stress conditions (Fig. 1): stress-free (disorganized fibril network), biaxial stress (disorganized fibril network), and uniaxial stress (aligned fibril network). These gels were cultured for 1, 2, or 3 weeks, resulting in nine unique groups. Samples were analyzed for cell viability, collagen fibril alignment, cellular morphology, proteoglycan content, biomarker production, and gene expression using histology, SCoRe microscopy, mass spectrometry and quantitative RT-PCR.

Cruciform Molds

Uniaxial and biaxial stress conditions were applied by casting cellular gel constructs into Teflon molds with a cruciform shape (Fig. 2a).²⁶ Teflon provides a highly hydrophobic surface that inhibits cell attachment. The cruciform molds were machined with a channel aspect ratio of 1:0.5. The larger arm width was 8 mm and the smaller arm width was 4 mm. Both arms had a length of 16 mm and a thickness of 5 mm. A 3 mm radius of curvature was machined at the corners to avoid tearing of the gel at mold corners. Glass rods were used as mechanical constraints against cell-driven gel compaction (Fig. 2b). These constraints caused the arms of the cruciform gel to experience a uniaxial stress condition and the center of the cruciform gel to experience a biaxial stress condition (Fig. 2a). The cruciform molds were machined to fit inside six-well plates (Fig. 2c). In addition, six-well plates without cruciform molds were used for a stress-free condition, where the diameter of the stress-free molds was 34.8 mm (Fig. 2d).

Cellular Collagen Gels

The collagen gel solution was produced by gently mixing 3 mg per mL of bovine collagen type I solution (Purecol[®], Advanced Biomatrix, San Diego, CA) in 10 \times high-glucose DMEM supplemented with 10% calf serum (CS) and 1% penicillin/streptomycin (100 I.U. penicillin/100 μ g/mL streptomycin (P/S)), and pH was adjusted to 7.4 with 0.1 M NaOH. The components were mixed in the following percentages: 53.7% Purecol[®], 13.9% 10 \times DMEM (with CS and P/S), 26.8% 1 \times PBS, and 5.6% 0.1 M NaOH. In order to prevent premature fibrillogenesis, the resulting solution was kept between 4 and 10 $^{\circ}$ C until seeded with cells.

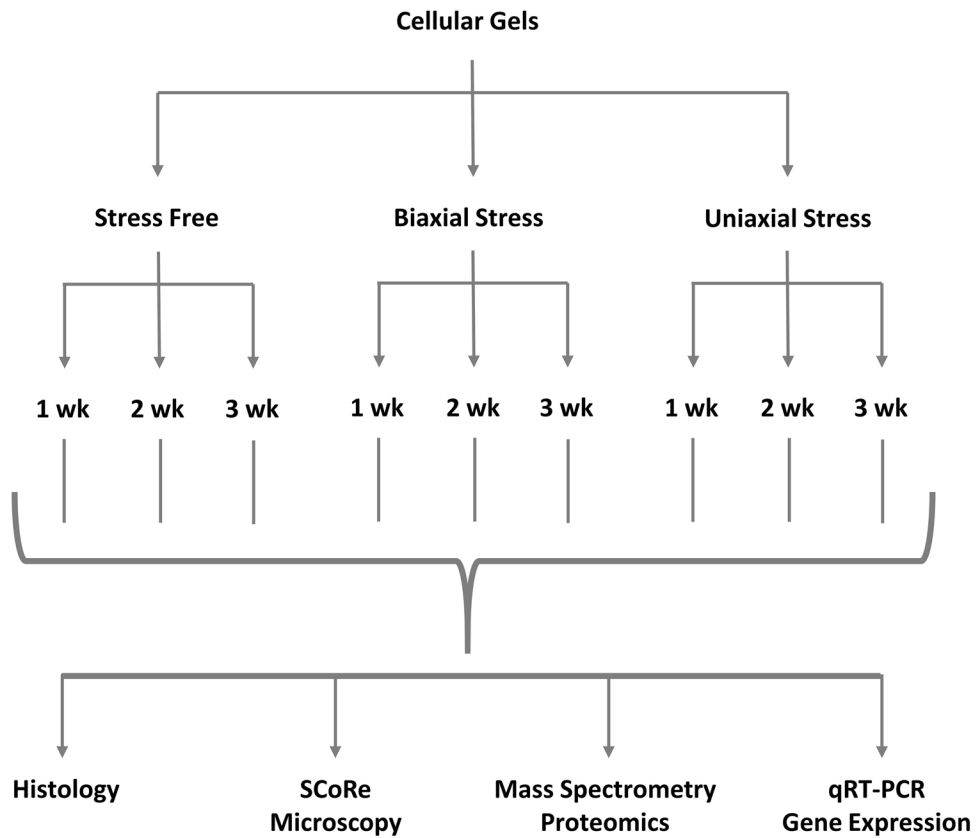


FIGURE 1. Overview of the experimental design. Collagen type I gels, seeded with mouse fibroblasts, were cultured under three static stress conditions. The gel extracellular matrix was analyzed at 1, 2, and 3-week time-points.

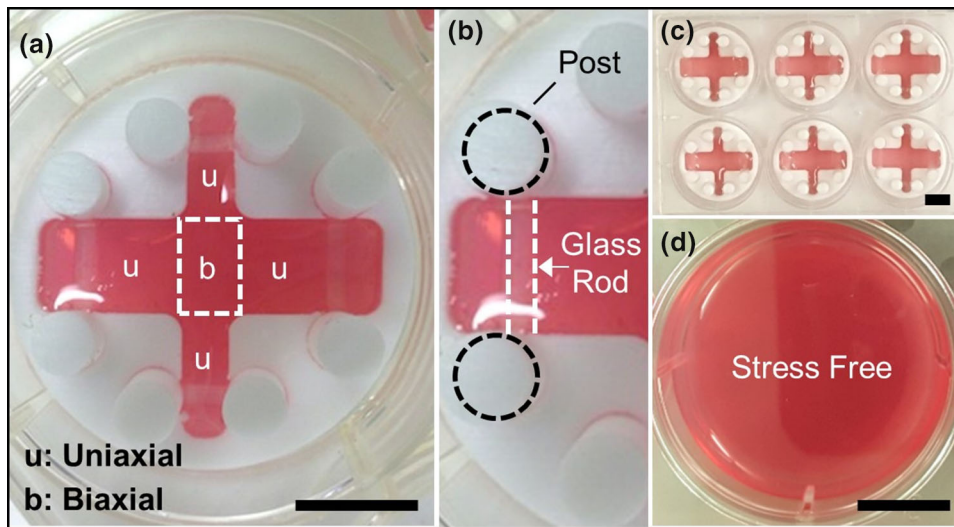


FIGURE 2. Cellular gels in molds. (a) Cruciform cellular gel with regions experiencing either uniaxial or biaxial stress. The dashed line indicates where a scalpel was used to separate the uniaxial and biaxial stressed regions for analysis. (b) A glass rod inserts into posts to provide mechanical constraint. (c) Six-well plate with cruciform molds. (d) Stress-free cellular gel from one well of a six-well plate. The pink area in each panel indicates the cellular gel. No media was added to the gels in these images. Scale bar on bottom right in panels (a), (c), and (d) is 10 mm.

The cell solution was produced using NIH-3T3 mouse embryonic fibroblasts (ATCC, Manassas, VA) maintained in high-glucose Dulbecco's Modified Eagle Medium (DMEM) supplemented with 10% CS and 1% P/S. NIH-3T3 cells are widely used as a model to investigate cellular response to mechanical load.^{7,15,40} Cells were cultured in a humidified incubator at 37 °C using 5% CO₂. When cells reached 60% confluency (every 3 days) they were passaged using trypsin/EDTA.

To make the cellular collagen gels, the NIH-3T3 cell solution was first added to the collagen gel solution in a ratio of ten parts collagen gel solution to 1 part cell solution, resulting in a final cellular density of 833,000 per mL. The cellular gel solution was then cast into the cruciform molds at 1.2 mL per mold (stressed specimen) or at 2 mL per well in six-well plates (stress-free specimen), and allowed to gel for 120 min in a tissue culture incubator at 37 °C. Cell culture media was added and exchanged every 3 days. Cruciform cellular gels and stress-free cellular gels were cast in six-well plates and were maintained in culture for time points of 1 week, 2 weeks and 3 weeks (Figs. 2c, 2d). A light/fluorescent microscope and calcein AM/trypan blue assay for live/dead cells was used to determine a minimum cell viability of 75% after 3 weeks of culture, which was consistent across all three static stress conditions. In total, 75 cruciform-shaped collagen gels and 45 stress-free collagen gels were synthesized, cultured, and analyzed. Prior to being analyzed, the uniaxial stressed and biaxial stressed regions of the cruciform-shaped collagen gels were separated by slicing with a scalpel. The separation line is at the transition of the uniaxial and biaxial stress regions, as demarcated by the dashed line in Fig. 2a.

Histology

Cellular gel specimens were fixed overnight in 10% formalin and then rinsed and stored in 35% ethanol until ready for embedding in paraffin. All gels were dehydrated, embedded in paraffin and sectioned at 8 μm. A minimum of 6 sections per gel were analyzed, two with Sirius red staining, two with haematoxylin and eosin staining, and two with Alcian blue staining. All staining was done following standard protocols.²⁷

Areas positive for Alcian blue staining were quantified using image processing functions in MATLAB (MathWorks, Natick, Massachusetts). For each test condition, four images from distinct regions were acquired. All images were identically cropped to analyze the central region and reduce edge effects. Images were converted to grayscale and then to a binary format using the MATLAB function *imbinarize* with manually selected global threshold values of 0.799 ± 0.37 . The MATLAB functions *imfill* and

bwareopen were used to eliminate small holes and reduce noise. The total number of selected pixels was divided by the total number of pixels in the cropped image to calculate the percent accumulation of proteoglycans in each image.²⁵ To verify the efficacy of this method, the outlines of the selected pixel groupings were superimposed on the original stained images and were qualitatively reviewed by the authors for accuracy (SMF, JTO, TJL). In addition, the PureCol collagen solution used in this study was internally tested to confirm that no proteoglycans were present. The Alcian blue analysis used three gels at each stress condition and time point, and four images were randomly acquired and analyzed in each group, for a total of 36 analyzed images.

SCoRe Microscopy

Spectral confocal reflectance microscopy (SCoRe),⁴¹ was used to evaluate the collagen fibril alignment in the uniaxial stress, biaxial stress and stress-free gels at each time point. The collagen gels were imaged using the 405 nm laser of a Zeiss 510 laser scanning confocal microscope and visualized using ZEN imaging software. Z-stack images were acquired with a Diode laser source (405 nm), a 63× Plan-Apochromat oil-immersion (NA 1.4) or 20× Plan-Apochromat (NA 0.8) objective, and an emission long pass filter of 505 nm.³¹ The three-dimensional z-stack was then projected onto a two-dimensional surface for analysis with FiberFit software.³² FiberFit applies a fast Fourier transform algorithm that measures fiber dispersion, expressed as a *k* value, where *k* is analogous to the reciprocal of variance in the fiber orientation distribution. Therefore, higher *k* values represent higher alignment of the fiber network. This SCoRe analysis used one sample at each stress condition and time point, and three sets of z-stacks were acquired per sample, for a total of 27 analyzed sets of z-stacks.

Mass Spectrometry

Proteins from the cellular gels were extracted using the RIPA buffer protocol (Millipore, Billerica, MA). Twenty micrograms of total protein from each sample was digested with Trypsin/Lys C mix (Promega, Madison, WI) following the manufacturer's instruction. Resulting peptide mixtures were chromatographically separated on a reverse-phase C18 column (10 cm × 75 μm, 3 μm, 120 Å) and analyzed on a Velos Pro Dual-Pressure Linear Ion Trap mass spectrometer (Thermo Fisher Scientific) as described previously.³⁹

Peptide spectral matching and protein identification were achieved by database search using Sequest HT algorithms in a Proteome Discoverer 1.4 (Thermo

Fisher Scientific). Raw spectrum data were searched against the UniProtKB/Swiss-Prot protein database for mouse (May 25, 2015) with the addition of bovine collagen $\alpha 1(I)$ sequence. Main search parameters included: trypsin, maximum missed cleavage site of two, precursor mass tolerance of 1.5 Da, fragment mass tolerance of 0.8 Da, and variable modification of oxidation/hydroxylation of methionine, proline, and lysine (+ 15.995 Da). A decoy database search was performed to calculate a false discovery rate (FDR). Proteins containing one or more peptides with $FDR \leq 0.05$ were considered positively identified and reported. For all targeted proteins (collagen $\alpha 1(I)$, collagen $\alpha 1(III)$, collagen $\alpha 1(V)$, integrin $\alpha 5$, tenascin-C, and decorin), the total number of peptide spectral matches (PSMs) reported by the Proteome Discoverer 1.4 was used for quantification. To identify newly synthesized mouse collagen $\alpha 1(I)$, and not preexisting bovine collagen, the number of PSMs from unique peptides for mouse was used for quantification. The mass spectrometry analysis used three samples at each stress condition and time point, for a total of 27 analyzed samples.

Gene Expression Analysis

RNA from each sample was extracted following the TRIzol protocol for RNA extraction (Thermo Fisher Scientific). Samples were flash-frozen with liquid nitrogen and then pulverized within the TRIzol reagent with an OMNI International TH homogenizer (Thomas Scientific). RNA concentration was determined by measuring the absorbance at 260 nm. The RT² First Strand Kit (Qiagen) was used for the generation of cDNA. Genes encoding biomarkers for healing or healthy ligament based on previously published work were amplified by quantitative real time PCR using a Roche Lightcycler 96 (Roche). These genes of interest were the genes encoding collagen $\alpha 1(I)$ chain (*Colla1*), collagen $\alpha 1(III)$ chain (*Col3a1*), collagen $\alpha 1(V)$ chain (*Col5a1*), integrin $\alpha 5$ (*Itga5*), and tenascin-C (*TnC*). The results were expressed as percent change (increase or decrease) compared to the expression of the housekeeping gene *GAPDH*, encoding glyceraldehyde-3-phosphate dehydrogenase. *GAPDH* was selected as the housekeeping gene for normalization in these experiments based on comparison to four other candidate housekeeping genes (*ActB*, *B2 m*, *Hsp90AB1*, and *GusB*) and was found to be stably expressed based on minimal variance. For this analysis the normalized $2^{-\Delta Ct}$ values were calculated. The gene expression analysis used sixteen samples at each time point for the uniaxial and biaxial stress condition, and six samples at each time point for the stress-free condition, for a total of 114 analyzed samples.

Statistical Analysis

Statistical analysis was performed in multiple parts using SPSS (Version 23; IBM Corp., Armonk, NY). The effect of stress condition and time on both gene expression results (*Colla1*, *Col3a1*, *Col5a1*, *Itga5*, *TnC*) and mass spectrometry results (collagen $\alpha 1(I)$, collagen $\alpha 1(III)$, decorin) were assessed using MANOVAs. The effect of stress condition and time on both fibril dispersion and area positive for Alcian blue staining was assessed using ANOVAs. For both MANOVA and ANOVA analyses, all pairwise comparisons were made using Bonferroni adjustments. Significance was set to $p < 0.05$, and all results are reported with standard deviation unless otherwise specified.

RESULTS

Collagen Organization

Collagen fiber organization was qualitatively examined by Sirius red staining of histological sections in each group of cellular gels (Fig. 3). The collagen fiber organization in the stress-free (Figs. 3a, 3b, and 3c) and biaxial (Figs. 3d, 3e, and 3f) cellular gels was disorganized. In contrast, the collagen fiber organization of the uniaxially stressed gels was highly aligned along the primary axis of tension (Figs. 3g, 3h, and 3i).

Collagen fibril organization was quantitatively evaluated by using SCoRe microscopy and FiberFit software to measure fibril dispersion k , for each group of cellular gels (Fig. 4). Stress-free (Figs. 4a, 4b, and 4c) and biaxial stress conditions (Figs. 4d, 4e and 4f) resulted in fibril networks with greater disorder than the uniaxial fibril network (Figs. 4g, 4h, and 4i; $p < 0.001$). No significant difference was found in fibril dispersion between the stress-free and biaxial stress conditions, and no significant differences in k values were observed as a function of time for any stress condition.

Cell Morphology

The morphology of NIH-3T3 fibroblasts in the collagen gels was qualitatively evaluated after hematoxylin and eosin staining of histological sections in each group of cellular gels (Fig. 5). The spindle shape morphology characteristic of fibroblasts was observed under each of the three static stress conditions. However, the fibroblasts in gels that experienced stress-free (Figs. 5a, 5b, and 5c) and biaxial loading (Figs. 5d, 5e, and 5f) had a less elongated appearance, possessing a more stellate characteristic. In comparison, the fibroblasts in the uniaxial stressed gels (Figs. 5g, 5h,

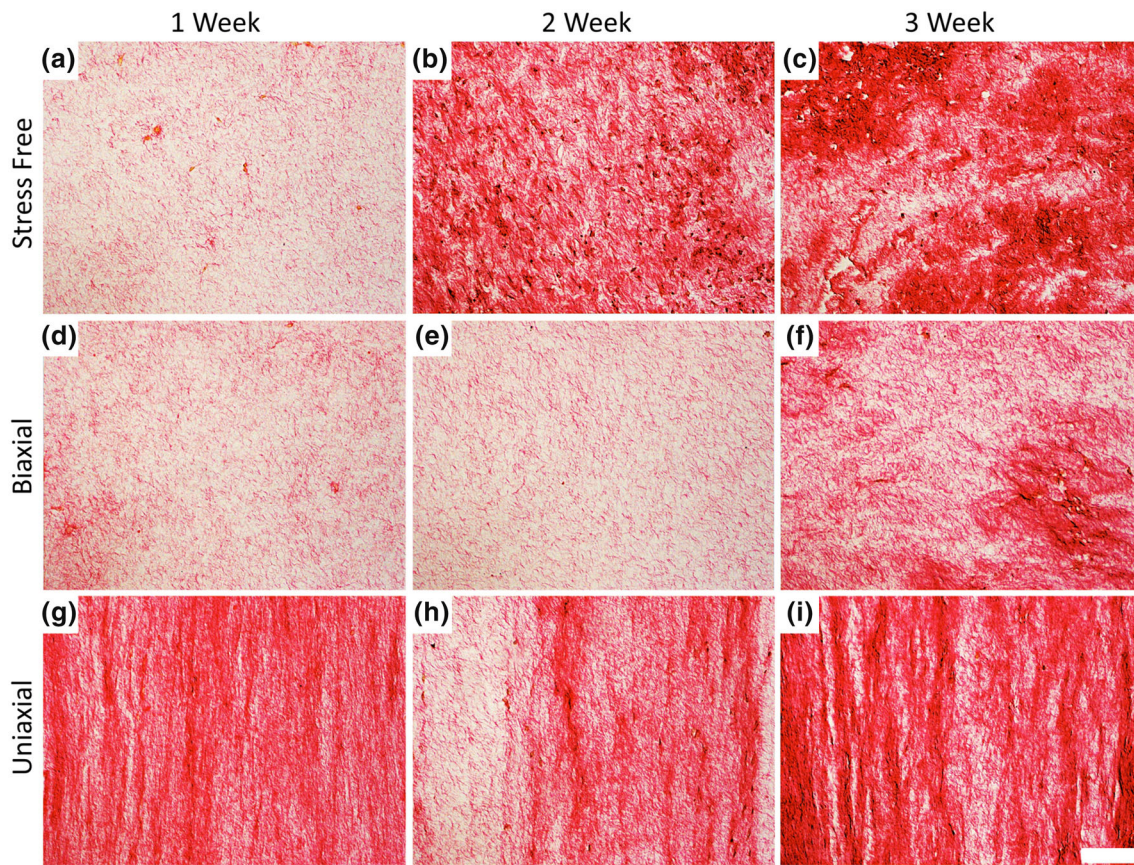


FIGURE 3. Photomicrograph from pico-Sirius red stained sections of cellular gels viewed with bright field microscopy. Gels were cultured under (a–c) stress-free, (d–f) biaxial stress and (g–i) uniaxial stress conditions at three time points. The bovine collagen type 1 fibers, from three-dimensional constructs, are stained deep red (this is not newly synthesized collagen). Scale bar on bottom right is 100 μm .

and 5i) appeared elongated along the primary axis of the collagen fibers and were spindle shaped.

Proteoglycan Accumulation

The level of proteoglycans synthesized by the resident fibroblasts and accumulated within the collagen gels was examined by Alcian blue staining of histological sections in each group of cellular gels (Fig. 6). Under stress-free conditions, proteoglycan accumulation increased by 30 times from week 1 to week 2 ($p < 0.001$), with no additional accumulation between week 2 and week 3 (Figs. 6a, 6b, and 6c). Biaxial loading had no significant increase in proteoglycans from week 1 to week 2, but increased by 4.6 times from week 1 to week 3 (Figs. 6d, 6e, and 6f; $p < 0.05$). Uniaxial loading had no significant increase in proteoglycans from week 1 to week 2, but increased by 21 times from week 1 to week 3 (Figs. 6g, 6h, and 6i; $p < 0.001$). At week 3, the proteoglycan accumulation under biaxial stress was significantly less than the other stress conditions ($p < 0.01$). A significant interaction

existed between time point and stress condition ($p < 0.001$).

Extracellular Matrix Protein Synthesis and Accumulation

Mass spectrometry was used to measure the relative abundance of proteins relevant to healing ligament in each group of cellular gels (Fig. 7). Collagen $\alpha 1(\text{I})$ was produced at a constant level and was not significantly affected by time or stress condition (Fig. 7a). Collagen $\alpha 1(\text{III})$ experienced a 93% decrease from week 1 to week 3 during stress-free loading, and experienced a 113% increase from week 1 to week 2 during uniaxial loading (Fig. 7b). At week 1, the uniaxial stress condition had the lowest production of collagen $\alpha 1(\text{III})$; and at week 3, the biaxial stress condition had the greatest production of collagen $\alpha 1(\text{III})$. Decorin levels showed a 152% increase from week 1 to week 2 during stress-free loading (Fig. 7c). At week 1 and week 2, the stress-free condition produced the greatest amount of decorin. A significant interaction existed between time

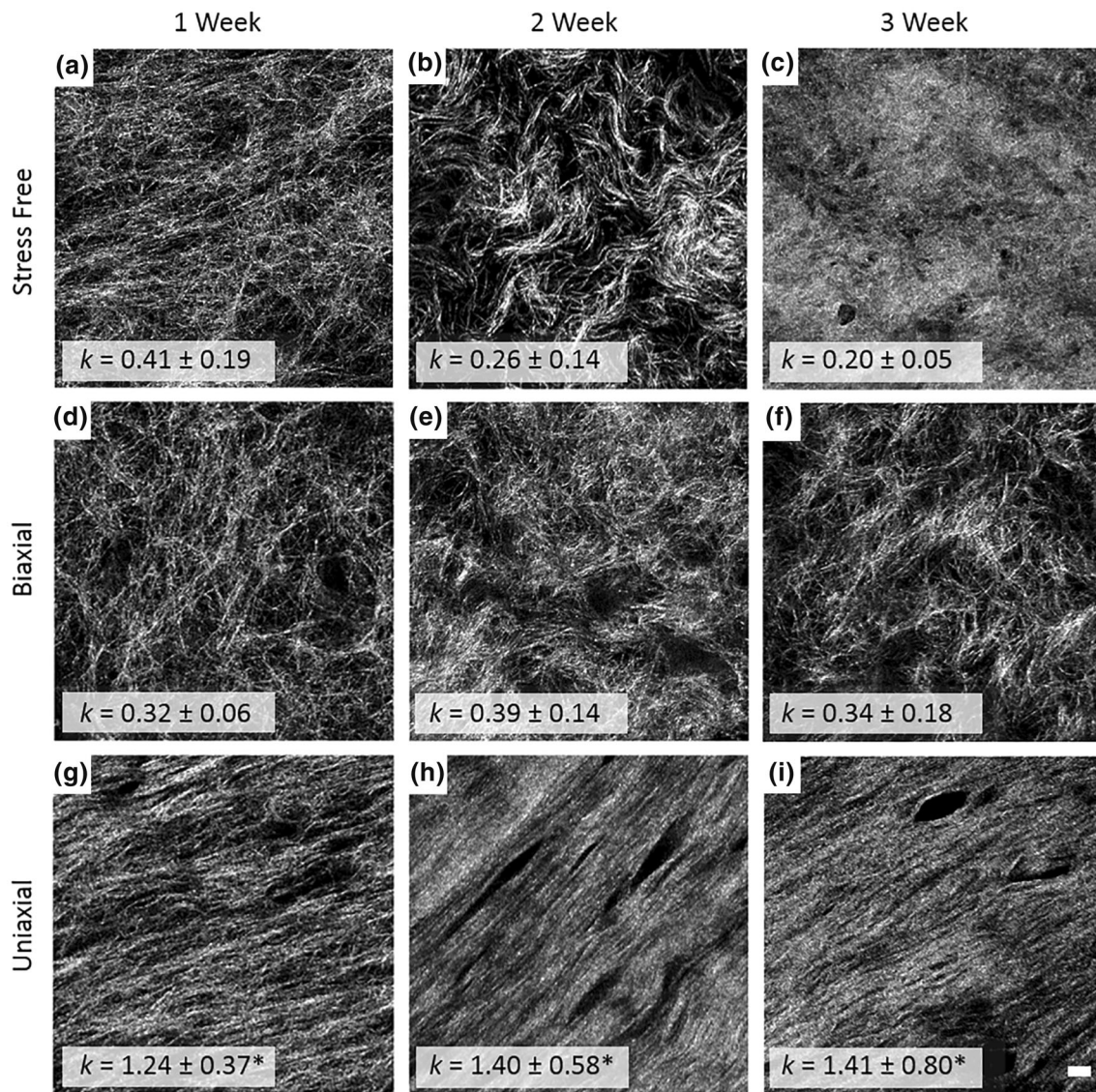


FIGURE 4. Cellular gels imaged using confocal microscopy at 63 \times and analyzed using FiberFit software to measure fiber dispersion k . Gels were cultured under (a–c) stress-free, (d–f) biaxial stress and (g–i) uniaxial stress conditions at three time points. The k values listed in each panel are averaged from nine confocal images. * = significantly greater k than biaxial and stress-free loading at the same time point. Scale bar on bottom right is 10 μm .

point and stress condition for both collagen $\alpha 1(\text{III})$ and decorin ($p < 0.001$). Other biomarkers related to healing ligament, including collagen $\alpha 1(\text{V})$ and integrin $\alpha 5$, did not have a detectable number of unique peptide spectral matches.

Gene Expression of Extracellular Matrix Constituents

The gene expression of molecules relevant to healing ligament was measured in each group of cellular gels (Fig. 8). Gene expression levels were not significantly

affected by stress condition in any of the five tested molecules. Gene expression levels were also unaffected by time point for *Coll1a1* (Fig. 8a), *Col5a1* (Fig. 8c), and *Itga5* (Fig. 8d). The *Col3a1* gene expression increased from week 1 to week 3 by 513% during stress-free loading, and increased by 42% during uniaxial loading (Fig. 8b). The *TnC* gene expression increased from week 1 to week 2 by 220% during stress-free loading (Fig. 8e). A significant interaction existed between time point and stress condition for *Col3a1* ($p < 0.01$).

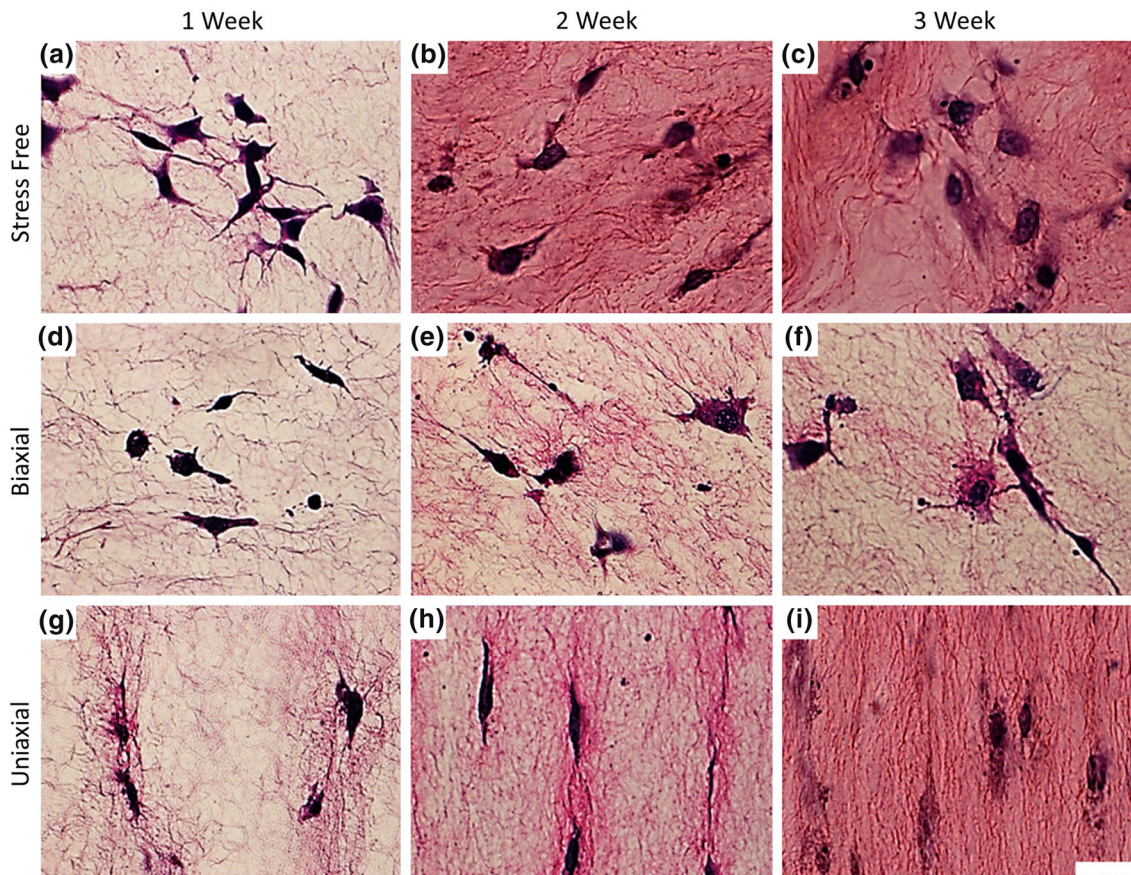


FIGURE 5. Photomicrograph of haematoxylin and eosin stained sections of cellular gels viewed with bright field microscopy. Qualitative differences in fibroblast cell morphology are observed between (a–c) stress-free, (d–f) biaxial stress and (g–i) uniaxial stress conditions across time points. Scale bar on bottom right is 20 μm .

DISCUSSION

The objective of this study was to determine the effect of static stress conditions on the expression and production of matrix molecules in fibroblast-cellular gels during culture. Our hypothesis was that fibroblasts in cellular-gels with disorganized fiber networks would produce biomarkers more representative of healing ligament than fibroblasts in cellular gels with aligned fiber networks. The biomarkers selected for analysis were based on previous *in vivo* studies that investigated fibroblast activity in healing ligament (Table 1).^{4,5,9,13,14,17,22,30,35,38,42}

These *in vivo* studies found that relative to healthy ligament tissue, a healing ligament that was 1–6 weeks post-injury had significant changes in the expression and/or production of the following matrix molecules: collagen type 1, collagen type 3, collagen type 5, integrin $\alpha 5$, tenascin-C, decorin, and proteoglycans (Table 1). The time points used for these *in vivo* studies

correspond to the formation of granulation tissue and early maturation into scar tissue.

The stress-free gels had time dependent changes in gene expression that best corresponded to early scar formation when compared to biaxial and uniaxial stressed gels. This included time dependent increases in gene expression for *Col3a1* and *TnC* (Fig. 8). However, the stress-free gels did not synthesize proteins similar to healing ligament, as decorin proteins increased over time and collagen type III proteins decreased over time (Fig. 7). It is possible that the reduction in collagen type III protein at each time point (Fig. 7b) may be a factor in the corresponding increases in *Col3a1* gene expression (Fig. 8b). Consistent with previous studies,⁶ the stress-free gels contracted during culture and this resulted in compaction of the extracellular molecules. This compaction can explain the observed increase in bovine collagen type I protein density over time (Fig. 3), and is one likely reason for the 30-fold increase in proteoglycan density

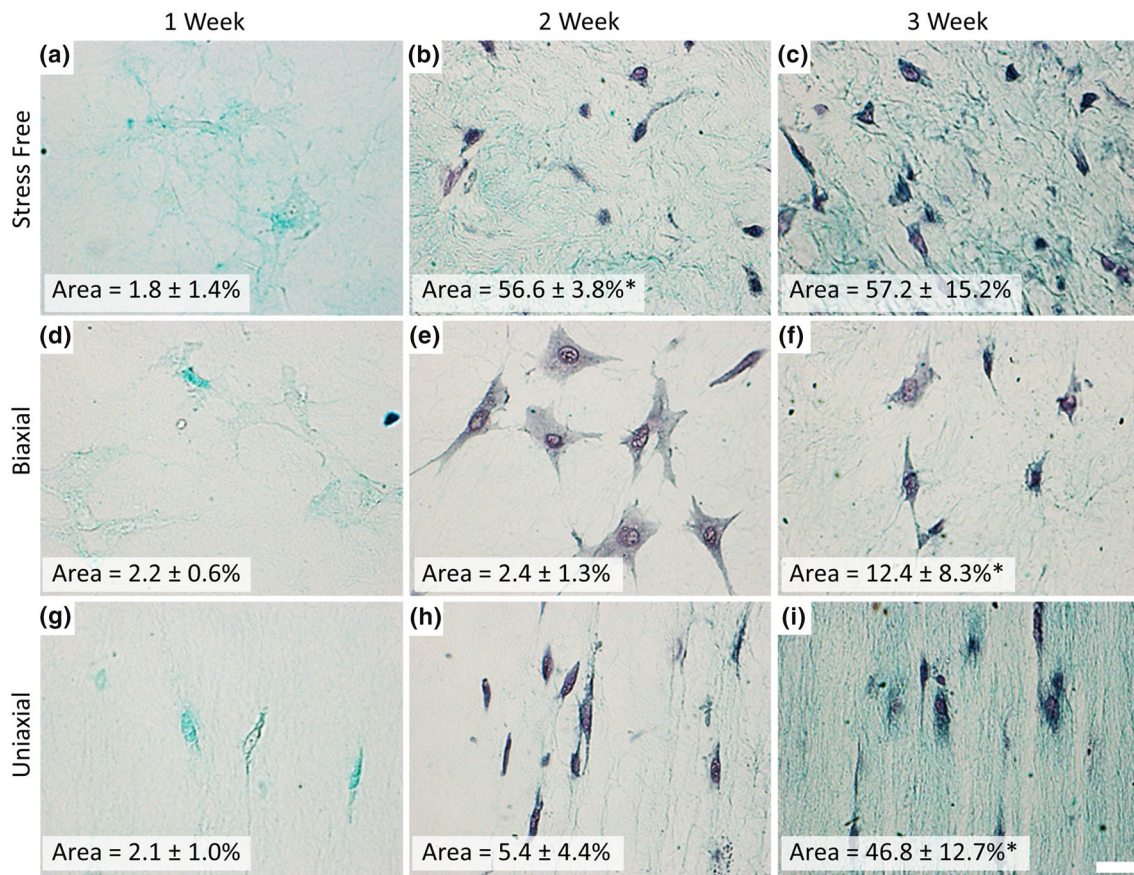


FIGURE 6. Photomicrograph of Alcian-blue stained sections of cellular gels viewed with bright field microscopy. The area of proteoglycan accumulation was analyzed in gels cultured under (a–c) stress-free, (d–f) biaxial stress and (g–i) uniaxial stress conditions at three time points. The area values listed in each panel were averaged from four images. * = significantly greater area than previous time point for the same stress condition. Scale bar on bottom right is 20 μm .

between week 1 and week 2 (Fig. 6). Uniform gel contraction of the stress-free gels also resulted in cells with a stellate like cell morphology with disorganized fiber organization that resembles early scar tissue.³⁴ Gel contraction may increase the number of cell–cell contacts,² and could play a role in modulating the different cellular responses observed between the three static stress conditions (Table 1).³

The biaxial stressed gels expressed protein levels that best corresponded to early scar formation when compared to stress-free and uniaxial gels (Table 1). This included an increase in collagen type III proteins at week 3, which was 20 times greater than the stress-free and uniaxial stressed gels (Fig. 7b), and less production of decorin than the stress-free gels (Fig. 7c). However, unlike the stress-free condition, biaxial stressed gels did not show increases in mRNA expression with time for any analyzed biomarker. Also, unlike the stress-free gels, the biaxial stressed gels resisted planar contraction, as is demonstrated by the lower density of collagen and proteoglycans in the biaxial stressed gels (Figs. 3, 5, 6). Proteoglycan

accumulation in both the uniaxial and biaxial stressed gels was delayed, indicating that static loading constraints inhibit fibroblast synthesis of proteoglycans.

As expected, the uniaxial stressed gels had a highly aligned collagen network with a fiber dispersion value, k , significantly greater than the stress-free and biaxial stressed gels (Fig. 4; greater k = greater fiber alignment). The strong collagen alignment in uniaxial stressed gels, and the observed spindle cell morphology (Fig. 5), is consistent with other studies that used a static uniaxial stress environment when culturing collagen gels,^{1,15} and is characteristic of healthy ligament. The uniaxial stressed gels were able to contract perpendicular to the loading axis, and therefore a high density of collagen was observed in the uniaxial stressed gels (Fig. 3).

The gene expression and protein production that we observed in the present study can be compared to previous research that used three-dimensional cellular hydrogel constructs. Previous proteomic research determined that collagen type I and collagen type III is abundant and highly expressed in fibroblast hydrogel

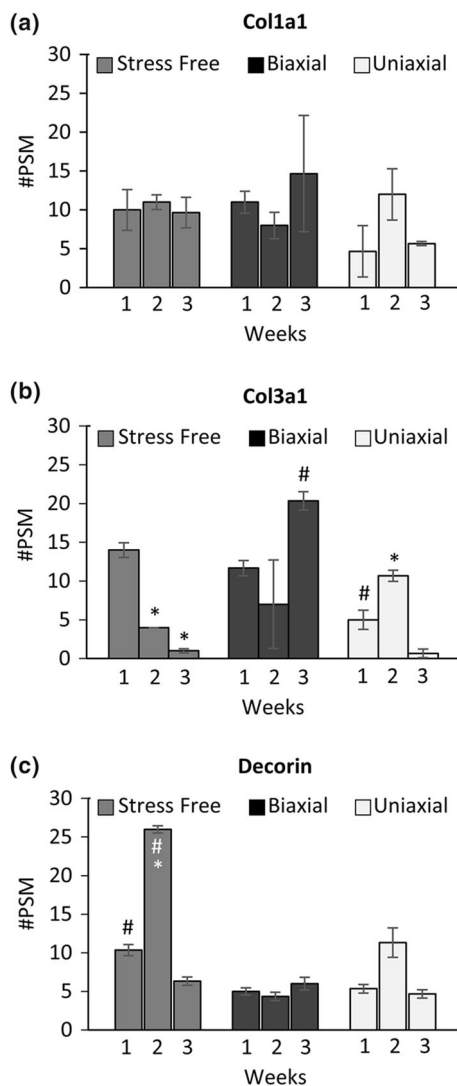


FIGURE 7. Relative protein abundance determined by Mass Spectrometry. Number of unique peptide spectral matches, #PSM, of (a) Collagen 1, (b) Collagen III, and (c) decorin in stress-free, biaxial stress and uniaxial stress conditions. * = significant change from the one-week time point within the same stress condition. # = significant change from the other stress conditions at the same time point. Error bars represent \pm standard error of the mean ($n = 3$).

constructs, but not at the same high level as native ligament tissue.^{26,28} Whereas primary human tenocytes cultured in fibrinogen-PGLA scaffolds for 4 weeks expressed genes for collagen type I and collagen type III at levels comparable to native tendon.⁴⁵ Our results build upon these findings by showing that the abundance and expression of collagen type I in fibroblast collagen gels is unaffected by culture time when subjected to uniaxial stress and biaxial stress (Figs. 7, 8), and only the stress-free condition had steady, yet insignificant, increases in collagen type I gene expression with time. Prior studies found that collagen type III is more highly expressed in ligament vs. tendon²⁸

and collagen type III protein content was increased in fibrin-based constructs seeded with primary fibroblasts from canine tendon and ligament that were stimulated with TGF- β 1.²¹ In the current study, collagen type III expression and production was time dependent, with the greatest protein production under biaxial stress (Fig. 7). A study by Henshaw *et al.* found that integrin α 5 expression in canine ACL fibroblast-collagen gels increases when subjected to static and dynamic tensile loads, compared to stress-free gels.²⁴ This differs from our results, which found no change in the low levels of *Itga5* expression between stress-free, biaxial, or uniaxial stressed gels. Kharaz *et al.* reported that decorin is present in fibroblast-collagen gels, albeit in less abundance than native tissue.²⁸ We also detected decorin production in all gels, with a sharp increase in decorin proteins at two-weeks in stress-free gels. *TnC* has previously been seen to be stimulated and produced in much higher levels in biaxial stressed gels with chick embryo fibroblasts when compared to the stress-free gels.¹² This is the opposite of what we see in our study, where *TnC* gene expression was significantly increased in the 2 week stress-free gels vs. the biaxial stressed gels. Differences could be attributed to the different cell lines (mouse vs. chick embryo) or the different time points (2 weeks vs. 2 days).

An interesting result of this study was that collagen organization was established within the first week of culture, and that no further significant changes were observed in collagen organization with time as the experiment progressed to week 2 and week 3 time points. Although there was a trend of increasing collagen disorder in the stress-free gels, the changes were not significant (Fig. 4; $p = 0.11$). These results indicate that any effect of gel contraction on collagen organization is negligible after week 1, and collagen organization is insensitive to fibroblast remodeling after week 1 for the subsequent 2 weeks of culture when exposed to static stress conditions. Therefore, there is limited benefit to culturing gels for more than 1 week when the goal is to establish a specific organization of the fibrillar constituents. However, cells may continue to respond to the established collagen organization over time beyond week 1.

Findings from the present study can provide guidelines for future studies that use fibroblast-collagen gels as *in vitro* models for ligament wound healing. To best replicate early scar tissue formation (Table 1), our results support initially culturing fibroblast-collagen gels for three-weeks under biaxial loading. At this time point, the gels will have a few biomarkers that correspond to early scar formation, including a disorganized collagen network, production of collagen type III, and low protein levels of decorin. These gels could then be subjected to chemical or mechanical treatments

Matrix Expression and Production in Fibroblast Gels

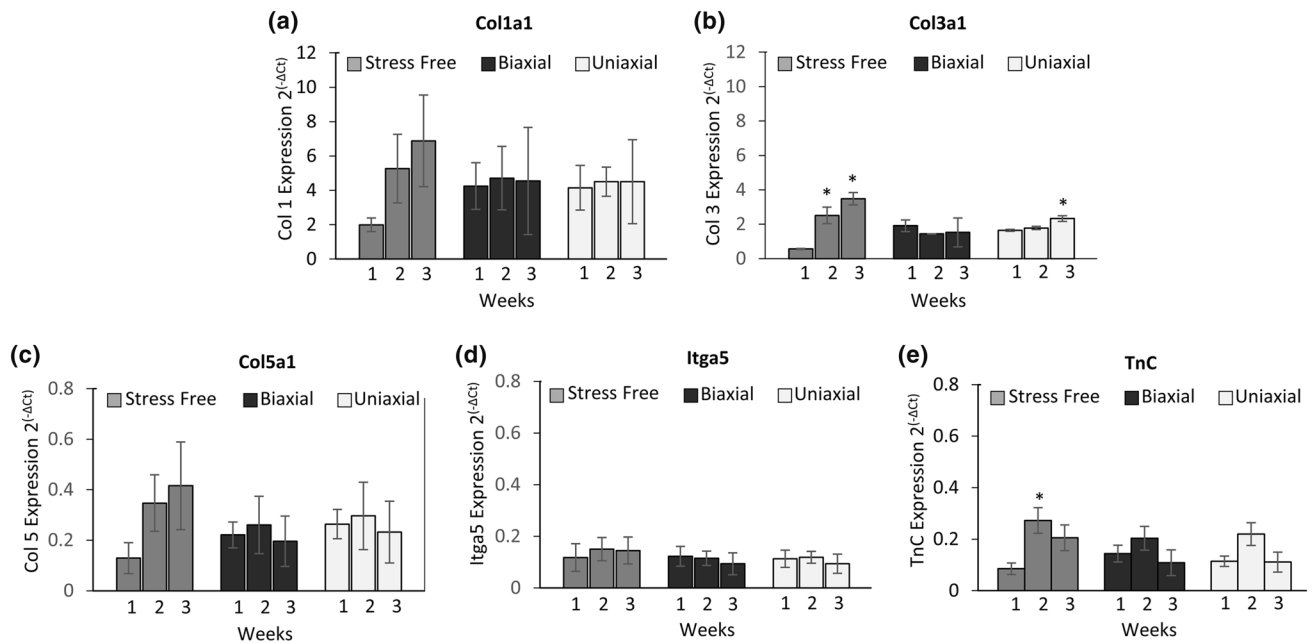


FIGURE 8. Gene expression determined by quantitative RT-PCR. Fold-change relative to the housekeeping gene, *GAPDH*, in (a) *Col1a1*, (b) *Col3a1*, (c), *Col5a1*, (d) *Itga5* (Integrin $\alpha 5$), and (e) *TnC* (Tenascin-C) in stress-free, uniaxial stress, and biaxial stress conditions over a three-week time course. * = significant change from the one-week time point within the same stress condition ($p < 0.05$). # = significant change from the other stress conditions at the same time point ($p < 0.05$). Error bars represent \pm standard error of the mean ($n = 3$).

of interest. For example, after the three-week culturing period, the biaxial gels could receive dynamic mechanical stimulations to investigate mechanobiological processes that promote the remodeling and alignment of disorganized collagen matrices. It is important to note that the recommendation to use a three-week culture time and a biaxial stressed condition may not be ideal for all applications. For instance, a stress-free gel may be better suited for studying a disorganized collagen network with higher densities of collagen and proteoglycans. Although the analysis of the cellular gels in this study does not measure many of the biological processes associated with healing ligament, such as angiogenesis,⁹ this study does provide for the first time a targeted evaluation of wound healing biomarkers in fibroblast-collagen gels. This quantitative comparison can serve as a baseline for future efforts to advance the development of an *in vitro* model for ligament wound healing.

Several study limitations should be mentioned. First, bovine collagen and mouse fibroblasts do not represent an exact model for human tissue. However, since collagens are highly conserved from species to species, a bovine collagen matrix is highly likely to reflect the structure of human and mouse collagen networks. Utilization of mouse fibroblasts with bovine collagen allowed us to distinguish newly synthesized collagen and other extracellular matrix constituents from the initial bovine matrix using peptide spectral

matching. NIH-3T3 cells are widely used as a model to investigate cellular response to mechanical load, and results of our study provide information about the response of fibroblasts to varied culture conditions. Second, the uniaxial and biaxial stressed gels were harvested from the same cruciform constructs. Although this design is advantageous in that it eliminates variability between the uniaxial and biaxial test groups, the close proximity between fibroblasts residing in the uniaxial and biaxial stressed regions of the cruciforms (Fig. 2) could result in intercellular signaling that alters the cell behavior in the different groups. Nevertheless, the millimeter scale of the gels would limit any artifact to a very small percentage of cells in the cruciform transition region (Fig. 2a, border of dashed rectangle). Diffusivity of extracellular biomatrix proteins from cells in the biaxial and uniaxial stressed regions can be quantified in future studies to examine the extent to which secreted proteins could provide short or long-distance induction and if cell behavior in the two groups is dependent upon the action of a signaling molecule produced in the adjacent region of the gel. Third, the cruciform had arms with different aspect ratios (Fig. 2a), and both arms were used for mRNA and protein analysis. Importantly, we detected no difference in fiber alignment between arms, therefore the difference in aspect ratios did not affect collagen organization. Fourth, similar to other studies that have characterized the molecular structure of cellular

TABLE 1. Comparison of biomarkers in healing ligament (from *in vivo* studies in literature) and biomarkers measured from cellular gels (present study).

Biomarker	Healing ligament		Gel (stress free)		Gel (biaxial stress)		Gel (uniaxial stress)	
	mRNA	Protein mass	mRNA	Protein mass ^a	mRNA	Protein mass ^a	mRNA	Protein mass ^a
Collagen I	↑↑ Boykiw <i>et al.</i> ⁴ Frank <i>et al.</i> ¹⁷	↓↓ Chamberlain <i>et al.</i> ^{9c}	=	=	=	=	=	=
Collagen III	↑↑ Boykiw <i>et al.</i> ⁴ Frank <i>et al.</i> ¹⁷ Martinez <i>et al.</i> ³⁰	↑↑ Chamberlain <i>et al.</i> ^{9c} Niyibizi <i>et al.</i> ^{35b}	↑	↓	=	↑	↑	↓
Collagen V	= Martinez <i>et al.</i> ³⁰	↑↑ Niyibizi <i>et al.</i> ^{35b}	=	nd	=	nd	=	nd
Integrin α -5	↓↓ Brune <i>et al.</i> ⁵	↑↑ Schreck <i>et al.</i> ^{42c}	=	nd	=	nd	=	nd
Tenascin-C	↑↑ Clements <i>et al.</i> ¹⁴	↑↑ Chockalingam <i>et al.</i> ^{13d}	↑	nd	=	nd	=	nd
Decorin	↓↓ Haslauer <i>et al.</i> ²² Martinez <i>et al.</i> ³⁰ Clements <i>et al.</i> ¹⁴	↓↓ Chamberlain <i>et al.</i> ^{9c} Plaas <i>et al.</i> ^{38b}	na	↑↑	na	=	na	=

↑↑ Significant change relative to healthy ligament from rabbit, rat, dog or human ($p < 0.05$).

↑ Significant change relative to both other loading conditions ($p < 0.05$).

↑ Significant change relative to time ($p < 0.05$).

= No significant change relative to time and/or loading condition.

na Data not acquired.

nd Data not detected.

^aMeasured with mass spectrometry.

^bMeasured with SDS-Page.

^cMeasured with immunohistochemistry.

^dMeasured with ELISA.

gels,^{1,12,24} the mechanical properties of the gels were not measured in this initial study. However, since a prior study using NIH-3T3 fibroblast-collagen gels reported a linear modulus of 50 kPa after 6 days of incubation,⁴⁰ which is 0.2% of the linear modulus of ligament one-week after injury,¹⁸ we can presume that the collagen gels used in the present study have inferior mechanical properties compared to healing ligament. Finally, not all biomarkers analyzed for mRNA expression were also analyzed for protein synthesis (Table 1) due to limits of detection with mass spectrometry. For example, collagen α 1(V) is an alpha chain of a minor fibrillar collagen found at low abundance in tissues, and in this study, no levels of collagen α 1(V) were detected at any time point.

In conclusion, this study provides for the first time a targeted evaluation of ligament wound healing biomarkers in fibroblast-collagen gels. We found that gels with disorganized collagen fibrils (stress-free and biaxial stress) better reproduced biomarkers that correspond to wound healing in ligament, relative to gels with highly aligned collagen fibrils (uniaxial stress).

Although these findings support our hypothesis, a considerable disparity existed between the matrix molecules expressed and produced during *in vivo* wound healing and in our fibroblast-collagen gels (Table 1). Future studies can build upon this work by determining external factors that promote the establishment of *in vitro* biomimetic systems for ligament wound healing. These model systems can serve as a research platform to develop therapies that restore the mechanical integrity of torn ligament.^{19,36}

ACKNOWLEDGMENTS

Authors wish to thank John Everingham for designing and assembling the cruciform, Laura Bond for statistical analysis, and Peter Martin for analysis of Alcian blue stained images. Authors acknowledge support by the Institutional Development Award (IDeA) Program from the National Institute of General Medical Sciences of the National Institutes of Health under Grants #P20GM103408 and

P20GM109095. We also acknowledge support from The Biomolecular Research Center at Boise State with funding from the National Science Foundation, Grants #0619793 and #0923535; the MJ Murdock Charitable Trust; Lori and Duane Steuckle, and the Idaho State Board of Education. Authors have no competing financial interests.

CONFLICT OF INTEREST

Authors have no competing financial interests.

REFERENCES

- ¹Akhouayri, O., M.-H. Lafage-Proust, A. Rattner, N. Laroche, A. Caillot-Augusseau, C. Alexandre, and L. Vico. Effects of static or dynamic mechanical stresses on osteoblast phenotype expression in three-dimensional contractile collagen gels. *J. Cell. Biochem.* 76:217–230, 2000.
- ²Bellows, C. G., A. H. Melcher, and J. E. Aubin. Contraction and organization of collagen gels by cells cultured from periodontal ligament, gingiva and bone suggest functional differences between cell types. *J. Cell Sci.* 50:299–314, 1981.
- ³Bloemen, V., T. Schoenmaker, T. J. De Vries, and V. Everts. Direct cell-cell contact between periodontal ligament fibroblasts and osteoclast precursors synergistically increases the expression of genes related to osteoclastogenesis. *J. Cell. Physiol.* 222:565–573, 2010.
- ⁴Boykiw, R., P. Sciore, C. Reno, L. Marchuk, C. B. Frank, and D. A. Hart. Altered levels of extracellular matrix molecule mRNA in healing rabbit ligaments. *Matrix Biol.* 17:371–378, 1998.
- ⁵Brune, T., A. Borel, T. W. Gilbert, J. P. Franceschi, S. F. Badylak, and P. Sommer. In vitro comparison of human fibroblasts from intact and ruptured ACL for use in tissue engineering. *Eur. Cell. Mater.* 14:71–78, 2007.
- ⁶Burgess, M. L., W. E. Carver, L. Terracio, S. P. Wilson, M. A. Wilson, and T. K. Borg. Integrin-Mediated Collagen Gel Contraction by Cardiac Fibroblasts Effects of Angiotensin II. *Circ. Res.* 74:291–298, 1994.
- ⁷Canović, E. P., D. T. Seidl, S. R. Polio, A. A. Oberai, P. E. Barbone, D. Stamenović, and M. L. Smith. Biomechanical imaging of cell stiffness and prestress with subcellular resolution. *Biomech. Model. Mechanobiol.* 13:665–678, 2014.
- ⁸Chamberlain, C. S., E. M. Crowley, H. Kobayashi, K. W. Eliceiri, and R. Vanderby. Quantification of collagen organization and extracellular matrix factors within the healing ligament. *Microanal. Microsc.* 17:779–787, 2011.
- ⁹Chamberlain, C. S., E. Crowley, and R. Vanderby. The spatio-temporal dynamics of ligament healing. *Wound Repair Regen.* 17:206–215, 2009.
- ¹⁰Chen, L. H., M. Warner, L. Fingerhut, and D. Makuc. Injury episodes and circumstances: National Health Interview Survey, 1997–2007. *Vital Health Stat.* 10. 1–55, 2009.
- ¹¹Chevallay, B., N. Abdul-Malak, and D. Herbage. Mouse fibroblasts in long-term culture within collagen three-dimensional scaffolds: Influence of crosslinking with diphenylphosphoryl azide on matrix reorganization, growth, and biosynthetic and proteolytic activities. *J. Biomed. Mater. Res.* 49:448–459, 2000.
- ¹²Chiquet-Ehrismann, R., M. Tarmheimer, M. Koch, A. Brunner, J. Spring, D. Martin, S. Baumgartner, and M. Chiquet. Tenascin-C expression by fibroblasts is elevated in stressed collagen gels. *J. Cell Biol.* 127:2093–2101, 1994.
- ¹³Chockalingam, P. S., S. S. Glasson, and L. S. Lohmander. Tenascin-C levels in synovial fluid are elevated after injury to the human and canine joint and correlate with markers of inflammation and matrix degradation. *Osteoarthr. Cartil.* 21:339–345, 2013.
- ¹⁴Clements, D. N., S. D. Carter, J. F. Innes, W. E. R. Ollier, and P. J. R. Day. Gene expression profiling of normal and ruptured canine anterior cruciate ligaments. *Osteoarthr. Cartil.* 16:195–203, 2008.
- ¹⁵Fernández, P., P. A. Pullarkat, and A. Ott. A master relation defines the nonlinear viscoelasticity of single fibroblasts. *Biophys. J.* 90:3796–3805, 2006.
- ¹⁶Foolen, J., S. L. Wunderli, S. Loerakker, J. G. Snedeker. Tissue alignment enhances remodeling potential of tendon-derived cells - Lessons from a novel microtissue model of tendon scarring. *Matrix Biol.* 65:14–29, 2018.
- ¹⁷Frank, C. B., D. A. Hart, and N. G. Shrive. Molecular biology and biomechanics of normal and healing ligaments—a review. *Osteoarthr. Cartil.* 7:130–140, 1999.
- ¹⁸Frank, C., S. L. Y. Woo, D. Amiel, F. Harwood, M. Gomez, and W. Akeson. Medial collateral ligament healing: a multidisciplinary assessment in rabbits. *Am. J. Sports Med.* 11:379–389, 1983.
- ¹⁹Gentleman, E., G. A. Livesay, K. C. Dee, and E. A. Nauman. Development of ligament-like structural organization and properties in cell-seeded collagen scaffolds in vitro. *Ann. Biomed. Eng.* 34:726–736, 2006.
- ²⁰Gomez, M. A., S. L. Woo, M. Inoue, D. Amiel, F. L. Harwood, and L. Kitabayashi. Medial collateral ligament healing subsequent to different treatment regimens. *J. Appl. Physiol.* 66:245–252, 1989.
- ²¹Hagerty, P., A. Lee, S. Calve, C. A. Lee, M. Vidal, and K. Baar. The effect of growth factors on both collagen synthesis and tensile strength of engineered human ligaments. *Biomaterials* 33:6355–6361, 2012.
- ²²Haslauer, C. M., B. L. Proffen, V. M. Johnson, and M. M. Murray. Expression of modulators of extracellular matrix structure after anterior cruciate ligament injury. *Wound Repair Regen.* 22:103–110, 2014.
- ²³Hauser, R. A. Ligament injury and healing: a review of current clinical diagnostics and therapeutics. *Open Rehabil. J.* 6:1–20, 2013.
- ²⁴Henshaw, D. R., E. Attia, M. Bhargava, and J. A. Hanafin. Canine ACL fibroblast integrin expression and cell alignment in response to cyclic tensile strain in three-dimensional collagen gels. *J. Orthop. Res.* 24:481–490, 2006.
- ²⁵Jensen, E. C. Quantitative analysis of histological staining and fluorescence using ImageJ. *Anat. Rec.* 296:378–381, 2013.
- ²⁶Jhun, C.-S., M. C. Evans, V. H. Barocas, and R. T. Tranquillo. Planar biaxial mechanical behavior of bioartificial tissues possessing prescribed fiber alignment. *J. Biomech. Eng.* 131:81006, 2009.
- ²⁷Junqueira, L. C. U., G. Bignolas, and R. R. Brentani. Picrosirius staining plus polarization microscopy, a specific method for collagen detection in tissue sections. *Histochem. J.* 11:447–455, 1979.
- ²⁸Kharaz, Y. A., S. R. Tew, M. Peffers, E. G. Canty-Laird, and E. Comerford. Proteomic differences between native

- and tissue-engineered tendon and ligament. *Proteomics* 16:1547–1556, 2016.
- ²⁹Loghmani, M. T., and S. J. Warden. Instrument-assisted cross-fiber massage accelerates knee ligament healing. *J. Orthop. Sport. Phys. Ther.* 39:506–514, 2009.
- ³⁰Martinez, D. A., A. C. Vailas, R. Vanderby, and R. E. Grindeland. Temporal extracellular matrix adaptations in ligament during wound healing and hindlimb unloading. *Am. J. Physiol. Integr. Comp. Physiol.* 293:R1552–R1560, 2007.
- ³¹Monici, M. Cell and tissue autofluorescence research and diagnostic applications. *Biotechnol. Annu. Rev.* 11:227–256, 2005.
- ³²Morrill, E. E., A. N. Tulepbergenov, C. J. Stender, R. Lamichhane, R. J. Brown, and T. J. Lujan. A validated software application to measure fiber organization in soft tissue. *Biomech. Model. Mechanobiol.* 15:1467–1478, 2016.
- ³³Murphy, P. G., B. J. Loitz, C. B. Frank, and D. A. Hart. Influence of exogenous growth factors on the synthesis and secretion of collagen types I and III by explants of expression of normal and healing rabbit ligaments. *Biochem. Cell Biol.* 72:403–409, 1994.
- ³⁴Nguyen, D. T., T. H. Ramwadhoebe, C. P. Van Der Hart, L. Blankevoort, P. P. Tak, and C. N. Van Dijk. Intrinsic healing response of the human anterior cruciate ligament: an histological study of reattached ACL remnants. *J. Orthop. Res.* 32:296–301, 2014.
- ³⁵Niyibizi, C., K. Kavalkovich, T. Yamaji, and S. L. Woo. Type V collagen is increased during rabbit medial collateral ligament healing. *Knee Surg. Sports Traumatol. Arthrosc.* 8:281–285, 2000.
- ³⁶Nöth, U., K. Schupp, A. Heymer, S. Kall, F. Jakob, N. Schütze, B. Baumann, T. Barthel, J. Eulert, and C. Hendrich. Anterior cruciate ligament constructs fabricated from human mesenchymal stem cells in a collagen type I hydrogel. *Cytotherapy* 7:447–455, 2005.
- ³⁷Pascher, A., A. F. Steinert, G. D. Palmer, O. Betz, J.-N. Gouze, E. Gouze, C. Pilapil, S. C. Ghivizzani, C. H. Evans, and M. M. Murray. Enhanced repair of the anterior cruciate ligament by in situ gene transfer: evaluation in an in vitro model. *Mol. Ther.* 10:327–336, 2004.
- ³⁸Plaas, A. H., S. Wong-Palms, T. Koob, D. Hernandez, L. Marchuk, and C. B. Frank. Proteoglycan metabolism during repair of the ruptured medial collateral ligament in skeletally mature rabbits. *Arch. Biochem. Biophys.* 374:35–41, 2000.
- ³⁹Pu, X., and J. T. Oxford. Proteomic analysis of engineered cartilage. *Methods Mol. Biol.* 1340:263–278, 2015.
- ⁴⁰Saddiq, Z. A., J. C. Barbenel, and M. H. Grant. The mechanical strength of collagen gels containing glycosaminoglycans and populated with fibroblasts. *J. Biomed. Mater. Res. Part A* 89:697–706, 2009.
- ⁴¹Schain, A. J., R. A. Hill, and J. Grutzendler. Label-free in vivo imaging of myelinated axons in health and disease with spectral confocal reflectance microscopy. *Nat. Med.* 20:443–449, 2014.
- ⁴²Schreck, P. J., L. R. Kitabayashi, D. Amiel, W. H. Akeson, and V. L. Woods. Integrin display increases in the wounded rabbit medial collateral ligament but not the wounded anterior cruciate ligament. *J. Orthop. Res.* 13:174–183, 1995.
- ⁴³Singer, A. J., and R. A. Clark. Cutaneous wound healing. *N. Engl. J. Med.* 341:738–746, 1999.
- ⁴⁴Stender, C. J., E. Rust, P. T. Martin, E. E. Neumann, R. J. Brown, and T. J. Lujan. Modeling the effect of collagen fibril alignment on ligament mechanical behavior. *Biomech. Model. Mechanobiol.* 17:543–557, 2018.
- ⁴⁵Stoll, C., T. John, M. Endres, C. Rosen, C. Kaps, B. Kohl, M. Sittinger, W. Ertel, and G. Schulze-Tanzil. Extracellular matrix expression of human tenocytes in three-dimensional air-liquid and PLGA cultures compared with tendon tissue: implications for tendon tissue engineering. *J. Orthop. Res.* 28:1170–1177, 2010.
- ⁴⁶van Rijn, R. M., A. G. van Os, R. M. D. Bernsen, P. A. Luijsterburg, B. W. Koes, and S. M. A. Bierma-Zeinstra. What is the clinical course of acute ankle sprains? A systematic literature review. *Am. J. Med.* 121(324–331):e7, 2008.